

## Dynamic Properties of Supercooled Chlorinated Biphenyls

A. P. Holt, D. Fragiadakis, and C. M. Roland\*

Cite This: *J. Phys. Chem. B* 2020, 124, 5073–5078

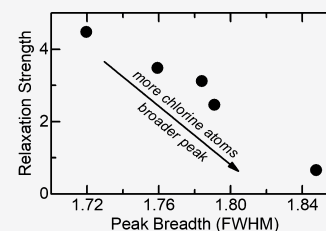
Read Online

ACCESS |

Metrics &amp; More

Article Recommendations

**ABSTRACT:** A study of the dynamics of a series of biphenyl compounds having varying chlorine levels was carried out. Increasing the chlorine content increases the glass transition temperature and makes the dynamics substantially more sensitive to density changes. Nonetheless, in the vicinity of their respective glass transitions, the different liquids display very similar extents of dynamic correlation and dynamic heterogeneity. The slight narrowing of the relaxation peak with increasing chlorine follows the general trend of the effect of increasing molecular polarity. This relationship between the peak breadth and dipole moment was reproduced in molecular dynamics simulations of a simplified model of the Aroclor molecule.



## INTRODUCTION

Glass formation is common to organic and inorganic liquids, ionic liquids, liquid crystals, metals, and polymers and as such remains an important problem from both a scientific and technological perspective. The dynamic properties of supercooled liquids exhibit many interesting behaviors, and crucial to “solving” the glass transition problem is to understand the relationship among these. The dynamics is inherently a many-body process, and therefore the expectation is that the dynamic properties are interrelated. Experimental determination of these correlations provides necessary groundwork for theoretical developments. A useful approach toward this end is to examine the properties within a chemical family or homologous series in order to isolate the key factors.

We present an experimental study of polychlorinated biphenyls (Aroclor from Monsanto), having the empirical formula  $C_{12}H_{10-n}Cl_n$  with  $n = 1-10$ . Aroclors are appealing for studying the relationship of the chemical structure of liquids to their relaxation properties: the glass transition temperature varies with chlorine content and the material is a mixture of congeners, which prevents crystallization. Substantial polarity and high electrical resistivity, in combination with thermal stability and low volatility, led to widespread application of Aroclors as electrical insulators in high-voltage transformers and capacitors and as heat transfer fluids;<sup>1,2</sup> these properties also make Aroclors well-suited for dielectric experiments. However, because of concerns about bioaccumulation and toxicity, particularly of biproducts of its thermal degradation, Aroclor production was discontinued in the late 1970s.<sup>3</sup>

This work extends previous studies<sup>4-8</sup> by examining the dynamics of a broader range of Aroclors. Supercooled liquids exhibit diverse properties, and the issue addressed herein is the interdependence of these properties. This is important because theories of glass transition usually focus on certain properties, for example, the non-Arrhenius behavior of the viscosity or relaxation time. A model making predictions for some

properties of vitrifying liquids should have the capacity to predict others, if the properties are correlated. This correlation may be absent if the characteristics have different origins but the problem of the glass transition is then considerably more complex. Of particular interest herein is the putative correlations of the distribution of relaxation times (relaxation dispersion breadth) with dynamic heterogeneity<sup>9</sup> and with the polarity or relaxation strength of a glass former.<sup>10-12</sup> Chlorinated biphenyls offer a test of these correlations within a single chemical family.

## EXPERIMENTAL SECTION

The five Aroclors studied here are listed in Table 1. Dielectric measurements were carried out on a Novocontrol Alpha-A analyzer and an IMass time domain dielectric analyzer over a frequency range of  $10^{-4}$  to  $10^6$  Hz. Samples were measured in

Table 1. Polychlorinated Biphenyls Studied Herein

name	avr. Cl atoms per molecule	$M_W$ (Da)	$T_g$ (K) ( $P = 0.1$ MPa)	$dT_g/dP^a$ (K/GPa)	$\gamma$	$\phi$
A1242	3	272	232.1	224	5.7	3.45
A1248	4	300	246.3	233	6.5	2.20
A1254	5	334	260.	321	6.9	2.83
A1260	6	378	275.	347	7.8	2.39
A1262	7	395	283.	317	9.3	1.97

<sup>a</sup>In the limit of low pressure, with  $T_g$  defined as the temperature at which  $\log \tau_\alpha$  (s) =  $-0.85$ .

Received: March 24, 2020

Revised: May 18, 2020

Published: May 20, 2020



a parallel plate geometry using stainless steel disc electrodes and Teflon spacers. To accurately determine the dielectric strength, the capacitance of the spacers was measured and subtracted from the spectra.

Temperature-modulated differential scanning calorimetry (TMDSC) employed a TA Q1000 with TA LNCS and was calibrated using indium and sapphire. For measurement of the absolute specific heat capacity of A1248 and A1260, samples were equilibrated at 50 °C, followed by cooling to −100 °C with an average cooling rate of 2.0 °C/min and a modulation of 0.32 C every 60 s. For A1242, A1254, and A1262, specific heat values were obtained from ref 4.

Volumetric experiments used a Gnomix instrument. For isothermal measurements, the pressure ranged from 10 to 200 MPa; for isobaric measurements, the temperature range was from 20 to 75 °C with a cooling rate of 0.5 °C/min.

We also carried out molecular dynamics simulations of a series of asymmetric dumbbell-shaped molecules with varying dipole moment, a simplified approximation of Aroclor to capture the general behavior. Simulations employed RUMD software<sup>13</sup> modified to incorporate a Berendsen barostat.<sup>14</sup> The systems studied are binary mixtures (1500:500, to avoid crystallization) of rigid, asymmetric dumbbell-shaped molecules AB (larger) and CD (smaller) in a cubic box. Atoms belonging to different molecules interact through the Lennard-Jones potential, using parameters based on the Kob–Andersen liquid.<sup>15</sup> Details of the parameters, procedure, and units used can be found in refs 16 and 17. We used a bond length of  $l = 0.6$  and a size ratio of the two particles comprising each molecule of  $r = 0.6$ . In addition, electrostatic interactions were computed using a simple cut-off at a distance of 4.5 units (for reference, the smallest simulation box length used was 11.7 units). Neglecting the long-range portion of the electrostatic interactions (rather than calculating them using, e.g., an Ewald summation) introduces a small systematic error; thus, we repeated the simulations with a reduced cut-off value of three units at selected state points to verify that the results are qualitatively the same and therefore, the truncation error is acceptably small. All quantities are expressed in dimensionless Lennard-Jones units. The thermostat (Nose–Hoover) and barostat had relaxation times of 0.2 and 2 units, respectively.

## RESULTS

The relaxation times of the Aroclors were measured as a function of temperature and pressure, with the pressure coefficient of the glass transition temperature,  $T_g$ , listed in Table 1. The sensitivity of  $T_g$  to pressure increases with increasing chlorine content. The relaxation times are shown in Figure 1 versus the specific volume,  $v(T,P)$ . The volume data, measured herein for A1248 and A1260 and taken from the literature for the other Aroclors,<sup>5</sup> were parameterized using the Tait equation of state<sup>18</sup>

$$v = v_0 \exp(\alpha_0) \left[ 1 - 0.0894 \ln \left( 1 + \frac{P}{b_0 \exp(-b_1 T)} \right) \right] \quad (1)$$

where  $\alpha_0$  is the isobaric thermal expansion coefficient at zero pressure and  $v_0$ ,  $b_0$ , and  $b_1$  are material constants. The best-fit values of these parameters are in Table 2.

We can collapse the data for each liquid onto a single curve using the density scaling equation, which describes dynamic and transport properties for normal liquids and polymers<sup>19,20</sup>

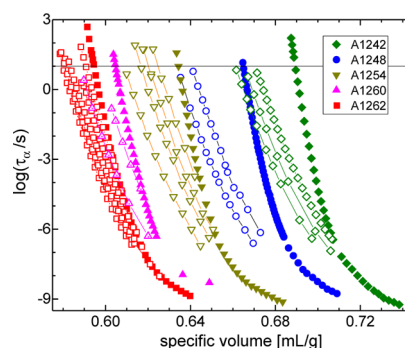


**Figure 1.** Relaxation times of Aroclors as a function of specific volume; solid symbols: ambient  $P$ ; open symbols: elevated  $P$ . The horizontal line indicates the effective  $T_g$ .

**Table 2.** Equation of State Parameters

	$v_0$ (mL/g)	$\alpha_0$ (C <sup>-1</sup> )	$b_0$ (GPa)	$b_1$ (C)
A1242	0.711 <sub>8</sub>	$6.57_2 \times 10^{-4}$	0.22 <sub>9</sub>	$4.89 \times 10^{-3}$
A1248	0.681 <sub>5</sub>	$6.75_6 \times 10^{-4}$	0.26 <sub>1</sub>	$4.72 \times 10^{-3}$
A1254	0.643 <sub>1</sub>	$6.59_2 \times 10^{-4}$	0.25 <sub>9</sub>	$5.24 \times 10^{-3}$
A1260	0.607 <sub>3</sub>	$4.16_5 \times 10^{-4}$	0.24 <sub>7</sub>	$4.38 \times 10^{-3}$
A1262	0.594 <sub>7</sub>	$7.00_9 \times 10^{-4}$	0.28 <sub>3</sub>	$5.20 \times 10^{-3}$

$$\tau = f(Tv^\gamma) \quad (2)$$

in which  $\gamma$  is a material constant. To apply eq 2, we used for the function  $f$  an equation derived from the Avramov model<sup>21</sup>

$$\tau = \tau_0 \exp\left(\frac{A}{Tv^\gamma}\right)^\phi \quad (3)$$

As seen in Figure 2, for relaxation times greater than 100 ns, the data are well-described by eq 3, with small deviations

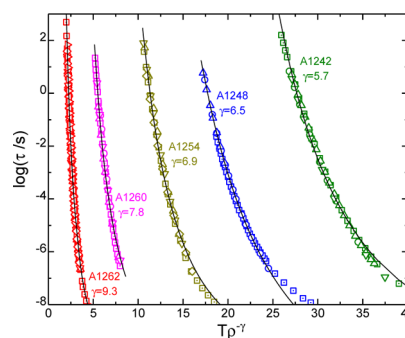


**Figure 2.** Density-scaled plots of the relaxation times, along with the fit of the equation, with the values for the scaling exponent shown.

apparent for  $\tau \leq 10^{-7}$  s. The latter likely reflects measurement errors at such high frequencies and limitations of the Avramov model. Nevertheless, the values determined for the scaling exponent should be accurate. There is a systematic increase in  $\gamma$  with chlorine content, mirroring the increase in the pressure coefficient of  $T_g$  (Table 1). An increasing effect of density on the dynamics implies a steeper intermolecular repulsive potential.<sup>22,23</sup>

Inferences regarding the intermolecular potential drawn from the magnitude of the scaling exponent are strictly valid only if the interactions are dominated by a spherically symmetric, pairwise additive, repulsive potential. However, the supercooled regime of liquids is defined by the growth of

many-body interactions, giving rise to complex, correlated dynamics. One consequence is that individual molecular mobilities vary, that is, there is a distribution of relaxation times, which broadens the relaxation peak. (A few experimental results<sup>24</sup> and a recent MD simulation<sup>25</sup> suggest that the connection between peak breadth and dynamic heterogeneity may be less direct.) This characteristic is expected to be related to other dynamic properties of supercooled liquids. For example, many published data (with some exceptions<sup>26</sup>) show that the relaxation time<sup>27,28</sup> and its temperature dependence<sup>29,30</sup> are both correlated with the breadth of the relaxation function. The temperature dependence is commonly

quantified by the fragility, defined as  $m = \left. \frac{d \ln \tau_\alpha}{d(T_g/T)} \right|_{T_g}$ . Prior

work found that the fragility for different Aroclors were equal to within a few percent,  $m \approx 60$ ,<sup>4,5</sup> implying comparable peak breadths.

An invariance of the shape of the  $\alpha$ -dispersion to temperature and pressure at a fixed value of the relaxation time,  $\tau$  (defined from the inverse of the peak frequency), is known as isochronal superpositioning.<sup>31,32</sup> In Figure 3, the  $\alpha$ -

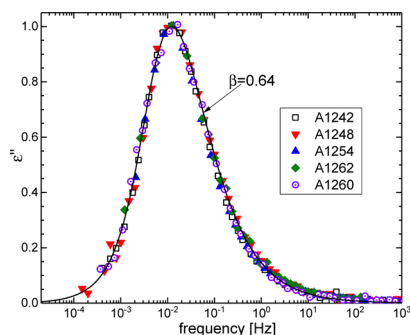


**Figure 3.** Dispersion in the dielectric loss for the five Aroclors, along with the fit of eq 4. The spectra have been normalized to superpose the peak maxima.

peaks of the five Aroclors, measured at different temperatures for which their peak frequencies were approximately equal, are seen to essentially superpose (after vertical shifts to account for differences in the respective dielectric strengths). There is an almost negligible change in the peak shape with chlorine content. This is an indication that any compositional heterogeneity inherent to Aroclors<sup>1</sup> has only a very minor effect on the peak breadth. However, the use of a graphical display to assess superpositioning entails problems—it is subjective and if the superpositioning is imperfect, the eye tends to be drawn to the peak maximum to the exclusion of the wings. This is further complicated by whether a linear or logarithmic ordinate scale is used, the latter possibly including contribution from any close-lying secondary peaks.

Accordingly, we fit the data in Figure 3 by the one-sided Fourier transform of the Kohlrausch function

$$\varepsilon(t) = \Delta\varepsilon \exp[-(t/\tau_\alpha)^\beta] \quad (4)$$

which yields  $\beta = 0.64 \pm 0.02$  at  $\tau = 100$  s. (For this value of  $\beta$ , the Kohlrausch relaxation time,  $\tau_\alpha$  in eq 4, is 20% smaller than  $\tau$  from the peak frequency.) Because the breadth of the  $\alpha$  peak decreases with increasing temperature ( $\beta$  changes about 0.01 per decade change of  $\tau$ ), the superpositioning in Figure 3 is not trivial. However, we can obtain a more accurate determination

of  $\beta$  by fitting the transform of eq 4 simultaneously to the real and imaginary components of the permittivity for each Aroclor spectrum. These results are shown in Table 3, and

**Table 3.** Dynamic Properties of Aroclors

	$\Delta c_p$ (J g <sup>-1</sup> K <sup>-1</sup> )	$\beta$	$N_c$	$\Delta\varepsilon$
A1242	0.26 <sub>9</sub>	0.66 <sub>3</sub>	399 ± 15	4.48
A1248	0.24 <sub>7</sub>	0.64 <sub>8</sub>	445 ± 42	3.48
A1254	0.22 <sub>4</sub>	0.63 <sub>9</sub>	412 ± 33	3.12
A1260	0.20 <sub>2</sub>	0.63 <sub>7</sub>	438 ± 59	2.46
A1262	0.19 <sub>4</sub>	0.61 <sub>7</sub>	386 ± 34	0.66

notwithstanding the ostensibly satisfactory superpositioning in Figure 3, there is a small, systematic increase in the peak breadth (smaller  $\beta$ ) with chlorine content of the Aroclor.

The cooperative dynamics of supercooled liquids manifest in a dynamic correlation length, that is, the spatial range over which the molecules exert reciprocal influences. This spatial variation of the dynamics is distinct from the variation of relaxation rates that gives rise to the distribution of relaxation times underlying the  $\alpha$ -peak breadth. Of course, the two effects have a related origin and for a given material have been found to be correlated,<sup>9,33</sup> however, there is no general relationship among different materials.<sup>9</sup> The dynamic correlation can be expressed in terms of the number of dynamically correlated molecules,  $N_c$ . A lower bound on  $N_c$  is obtained using the formula<sup>34</sup>

$$N_c = \frac{k_B}{\Delta c_p} \left( \frac{\beta}{e} \right)^2 \left( \frac{d \ln \tau_\alpha}{d \ln T} \right)^2 \quad (5)$$

which is most accurate near  $T_g$ . In this equation,  $k_B$  is the Boltzmann constant,  $e$  is Euler's number, and  $\Delta c_p$  is the isobaric heat capacity change at the glass transition. We calculate  $N_c$  near  $T_g$  for the five Aroclors, with the values of  $\Delta c_p$  given in Table 3. As seen in Figure 4,  $N_c$  is constant within the

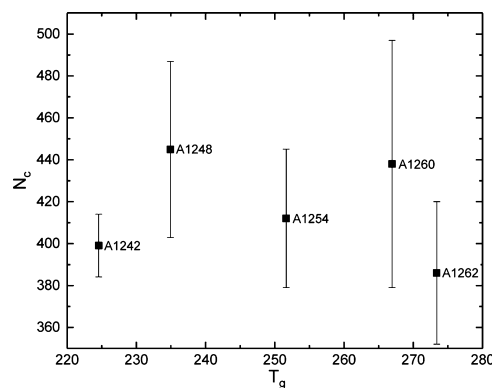


**Figure 4.** Number of dynamically correlated molecules estimated from eq 5 for the five Aroclors.

(large) uncertainty. Thus, for the Aroclors at fixed  $\tau$ , the two measures of intermolecular cooperativity, the distribution of relaxation times and the dynamic correlation volume, are both at most only weakly dependent on the chemical structure of the Aroclor.

The simultaneous fitting of the real and imaginary components of the dielectric spectra also yields the dielectric strengths,  $\Delta\varepsilon$  (Table 3). There is small but significant variation in  $\Delta\varepsilon$  for the Aroclors. From analysis of copious literature data

for van der Waals materials, the width of the  $\alpha$ -loss peak in the vicinity of  $T_g$  was found to be anticorrelated with the polarity of the molecule.<sup>10,11</sup> In Figure 5,  $\Delta\epsilon$  versus  $\beta$  is plotted for the

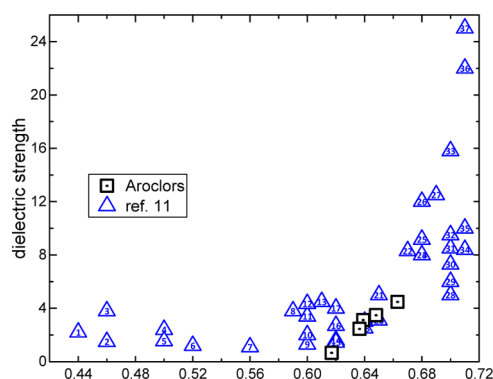


**Figure 5.**  $\Delta\epsilon$  as a function of  $\beta$  for the five Aroclors; the values are consistent with the behavior of a broad range of liquids reported in the literature.<sup>11</sup>

Aroclors, with literature values from ref 11 included (these materials are identified in Table 4). It can be seen that the

**Table 4. Materials in Figure 5 (from ref 11)**

1	Ethylbenzene
2	Carvedilol
3	dicyclohexyl-2-methylsuccinate
4	itraconazole
5	Posnaconazole
6	Azithromycin
7	triphenyl phosphite
8	Indomethacin
9	$\beta$ -pentaacetylglucose
10	biphenyl-2-isobutylate
11	$\alpha$ -phenyl- <i>o</i> -cresol
12	$\beta$ -adenosine
13	Telimisartan
14	Roxithromycin
15	1,1'-bis( <i>p</i> -methoxyphenyl)cyclohexane
16	Clarithromycin
17	$\alpha$ -pentaacetylglucose
18	Rofecoxib
19	dimethyl phthalate
20	dipropylene glycol dibenzoate
21	dioctyl phthalate
22	Celecoxib
23	Eugenol
24	Sildenafil
25	$\beta$ -thymidine
26	$\beta$ -uridine
27	benzoyn butylether
28	2,3-epoxypropyl phenylether
29	Ketoprofen
30	methyl- <i>m</i> -toluate
31	Fenofibrate
32	Ezetimibe
33	Isocyanocyclohexane
34	diethyl phthalate
35	Ranolazyna
36	3-bromopentane
37	diphenyl-vinylene carbonate

Aroclor data are consistent with a general relationship of increasing  $\Delta\epsilon$  with increasing  $\beta$ . This result is in contrast to an interpretation of the peak breadth in terms of the strength of the intermolecular coupling, whereby broader peaks (smaller  $\beta$ ) reflect stronger steric hindrances and interactions among neighboring molecules.<sup>19</sup> One might anticipate that given the limited flexibility of the biphenyl moiety, pendant chlorine atoms would hinder rotation of the phenyl rings, with the nonplanar structure of Aroclor engendering stronger steric impediments to local motion, thus broadening the dispersion. This is not the case; evidently, the role of intermolecular cooperativity and the distribution of relaxation times reflected in  $\beta$  bears further scrutiny.

In an earlier study, we compared the effect of a dipole moment on isochronal superpositioning and density scaling of simulated methanol.<sup>35</sup> Analyzing those data, we find that the introduction of a dipole moment of 1.9D narrows the dispersion in comparison to the nonpolar compound, with  $\beta$  increasing from  $\sim 0.6$  to a value around 0.7. Herein, we carried out molecular dynamics simulations on a simplified Aroclor structure, mixtures of asymmetric dumbbells (similar to the real material, mixtures are required to suppress crystallization). The dipole moment was systematically varied and a stretched exponential function fit to the first-order rotational correlation function

$$C(t) = \langle \cos \theta(t) \rangle \quad (6)$$

where  $\theta$  is the angular change of a unit vector along the molecular axis. Results are shown in Figure 6 for  $P = 1.0$  and at

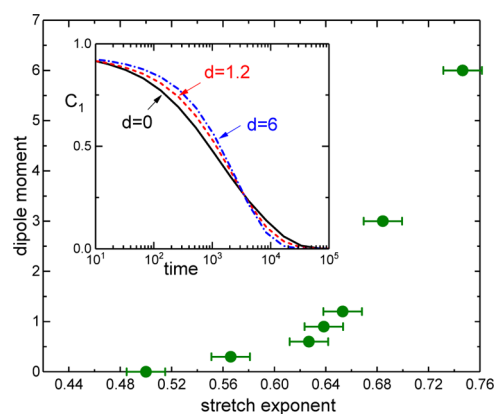


**Figure 6.** Dipole moment as a function of  $\beta$  for the simulated asymmetric dumbbell molecules. The inset shows the first-order rotational correlation function for the indicated values of  $d$ . For all points shown, pressure is  $P = 1$  and temperatures are  $T = 0.36, 0.35, 0.35, 0.37, 0.41, 0.76,$  and  $1.86$  in the order of increasing dipole moment.

a constant value of the relaxation time ( $\log \tau = 3.3 \pm 0.1$ ), where it is evident that an increase in the molecular polarity causes the dispersion to narrow. The behavior is qualitatively the same as observed for real Aroclor.

## CONCLUSIONS

The dynamic properties of a series of chlorinated biphenyl compounds were measured. With increasing chlorine, there is a substantial increase in the influence of density on the dynamics, relative to the effect of temperature. This can be seen in the systematically larger density scaling exponent, from  $\gamma = 5.7$  for A1242 to a value of 9.3 for A1262. However, the

influence of intermolecular cooperativity of the dynamics is only very modestly affected by the chlorine content. At  $T_g$ , both the distribution of relaxation times and the number of dynamically correlated molecules are almost invariant. In fact, the Kohlrausch stretch exponent *increases* with chlorine content, as the relaxation peak slightly narrows. As found very generally and affirmed herein from molecular dynamics simulations, the breadth of the peak is anticorrelated with the strength of the Aroclor dipole moment.

## AUTHOR INFORMATION

### Corresponding Author

C. M. Roland – Chemistry Division, Code 6105, Naval Research Laboratory, Washington, D.C. 20375-4032, United States;

orcid.org/0000-0001-7619-9202; Email: croland52@gmail.com

### Authors

A. P. Holt – Chemistry Division, Code 6105, Naval Research Laboratory, Washington, D.C. 20375-4032, United States;

orcid.org/0000-0003-2916-6963

D. Fragiadakis – Chemistry Division, Code 6105, Naval Research Laboratory, Washington, D.C. 20375-4032, United States; orcid.org/0000-0002-0259-3677

Complete contact information is available at:  
<https://pubs.acs.org/10.1021/acs.jpcc.0c02601>

### Notes

The authors declare no competing financial interest.

## ACKNOWLEDGMENTS

A.P.H. acknowledges an American Society for Engineering Education postdoctoral fellowship. This work was supported by the Office of Naval Research.

## REFERENCES

- (1) Penning, C. H. Physical characteristics and commercial possibilities of chlorinated diphenyl. *Ind. Eng. Chem.* **1930**, *22*, 1180–1182.
- (2) Erickson, M. D.; Kaley, R. G. Applications of polychlorinated biphenyls. *Environ. Sci. Pollut. Res. Int.* **2011**, *18*, 135–151.
- (3) Robertson, L. W.; Ludwig, G. Polychlorinated Biphenyl (PCB) carcinogenicity with special emphasis on airborne PCBs. *Gefahrstoffe—Reinhalt. Luft* **2011**, *71*, 25–32.
- (4) Roland, C. M.; Casalini, R. Enthalpy relaxation and fragility in polychlorinated biphenyls. *J. Therm. Anal. Calorim.* **2006**, *83*, 87–90.
- (5) Roland, C. M.; Casalini, R. Effect of chemical structure on the isobaric and isochoric fragility in polychlorinated biphenyls. *J. Chem. Phys.* **2005**, *122*, 134505.
- (6) Casalini, R.; Roland, C. M.  $\alpha$ -relaxation and the excess wing in polychlorinated biphenyls. *Phys. Rev. B: Condens. Matter Mater. Phys.* **2002**, *66*, 180201.
- (7) Casalini, R.; Paluch, M.; Roland, C. M. Correlation between the alpha relaxation and the excess wing for polychlorinated biphenyls and glycerol. *J. Therm. Anal. Calorim.* **2002**, *69*, 947–952.
- (8) Casalini, R.; Paluch, M.; Fontanella, J. J.; Roland, C. M. Investigation of the correlation between structural relaxation time and configurational entropy under high pressure in a chlorinated biphenyl. *J. Chem. Phys.* **2002**, *117*, 4901.
- (9) Roland, C. M.; Fragiadakis, D.; Coslovich, D.; Capaccioli, S.; Ngai, K. L. Correlation of nonexponentiality with dynamic heterogeneity from four-point dynamic susceptibility  $\chi(4)(t)$  and its approximation  $\chi(T)(t)$ . *J. Chem. Phys.* **2010**, *133*, 124507.
- (10) Jedrzejowska, A.; Wojnarowska, Z.; Adrjanowicz, K.; Ngai, K. L.; Paluch, M. Toward a better understanding of dielectric responses

of van der Waals liquids: The role of chemical structures. *J. Chem. Phys.* **2017**, *146*, 094512.

(11) Paluch, M.; Knapik, J.; Wojnarowska, Z.; Grzybowski, A.; Ngai, K. L. Universal behavior of dielectric responses of glass formers: role of dipole-dipole interactions. *Phys. Rev. Lett.* **2016**, *116*, 025702.

(12) Gainaru, C. Spectral shape simplicity of viscous materials. *Phys. Rev. E* **2019**, *100*, 020601.

(13) Bailey, N.; Ingebrigtsen, T.; Hansen, J. S.; Veldhorst, A.; Bohling, L.; Lemarchand, C.; Olsen, A.; Bacher, A.; Costigliola, L.; Pedersen, J.; Larsen, H.; Dyre, J.; Schroder, T. RUMD: A general purpose molecular dynamics package optimized to utilize GPU hardware down to a few thousand particles. *SciPost Phys.* **2017**, *3*, 038.

(14) Berendsen, H. J.; Postma, V.; van Gunsteren, W. F.; DiNola, A. R. H. J.; Haak, J. R. Molecular dynamics with coupling to an external bath. *J. Chem. Phys.* **1984**, *81*, 3684.

(15) Kob, W.; Andersen, H. C. Scaling Behavior in the  $\beta$ -Relaxation Regime of a Supercooled Lennard-Jones Mixture. *Phys. Rev. Lett.* **1994**, *73*, 1376.

(16) Fragiadakis, D.; Roland, C. M. Molecular dynamics simulation of the Johari-Goldstein relaxation in a molecular liquid. *Phys. Rev. E: Stat., Nonlinear, Soft Matter Phys.* **2012**, *86*, 020501.

(17) Fragiadakis, D.; Roland, C. M. Rotational dynamics of simple asymmetric molecules. *Phys. Rev. E: Stat., Nonlinear, Soft Matter Phys.* **2015**, *91*, 022310.

(18) Zoller, P.; Walsh, D. J. *Standard Pressure-Volume-Temperature Data for Polymers*; Technomic: Lancaster, PA, 1995.

(19) Roland, C. M.; Hensel-Bielowka, S.; Paluch, M.; Casalini, R. Supercooled dynamics of glass-forming liquids and polymers under hydrostatic pressure. *Rep. Prog. Phys.* **2005**, *68*, 1405–1478.

(20) Roland, C. M. *Viscoelastic Behavior of Rubbery Materials*; Oxford University Press: Oxford, 2011.

(21) Casalini, R.; Mohanty, U.; Roland, C. M. Thermodynamic interpretation of the scaling of the dynamics of supercooled liquids. *J. Chem. Phys.* **2006**, *125*, 014505.

(22) Coslovich, D.; Roland, C. M. Thermodynamic scaling of diffusion in supercooled Lennard-Jones liquids. *J. Phys. Chem. B* **2008**, *112*, 1329–1332.

(23) Roland, C. M.; Bair, S.; Casalini, R. Thermodynamic scaling of the viscosity of van der Waals, H-bonded, and ionic liquids. *J. Chem. Phys.* **2006**, *125*, 124508.

(24) Koperwas, K.; Grzybowski, A.; Grzybowska, K.; Wojnarowska, Z.; Sokolov, A. P.; Paluch, M. Effect of temperature and density fluctuations on the spatially heterogeneous dynamics of glass-forming van der waals liquids under high pressure. *Phys. Rev. Lett.* **2013**, *111*, 125701; Erratum: Effect of temperature and density fluctuations on the spatially heterogeneous dynamics of glass-forming van der waals liquids under high pressure. *Phys. Rev. Lett.* **2014**, *113*, 069901.

(25) Hung, J.-H.; Mangalara, J. H.; Simmons, D. S. Heterogeneous rouse model predicts polymer chain translational normal mode decoupling. *Macromolecules* **2018**, *51*, 2887–2898.

(26) Zhang, X.; Zhao, J.; Ye, C.; Lai, T.-Y.; Snyder, C. R.; Karim, A.; Cavicchi, K. A.; Simmons, D. S. Dynamical correlations for statistical copolymers from high-throughput broad-band dielectric spectroscopy. *ACS Comb. Sci.* **2019**, *21*, 276–299.

(27) Roland, C. M.; Casalini, R.; Paluch, M. Isochronal temperature-pressure superpositioning of the alpha-relaxation in type-A glass formers. *Chem. Phys. Lett.* **2003**, *367*, 259–264.

(28) Ngai, K. L.; Casalini, R.; Capaccioli, S.; Paluch, M.; Roland, C. M. Do theories of the glass transition, in which the structural relaxation time does not define the dispersion of the structural relaxation, need revision? *J. Phys. Chem. B* **2005**, *109*, 17356–17360.

(29) Böhmer, R.; Ngai, K. L.; Angell, C. A.; Plazek, D. J. Nonexponential relaxations in strong and fragile glass formers. *J. Chem. Phys.* **1993**, *99*, 4201–4209.

(30) Ngai, K. L.; Roland, C. M. Chemical structure and intermolecular cooperativity - Dielectric relaxation results. *Macromolecules* **1993**, *26*, 6824–6830.

(31) Hansen, H. W.; Frick, B.; Capaccioli, S.; Sanz, A.; Niss, K. Isochronal superposition and density scaling of the  $\alpha$ -relaxation from pico- to millisecond. *J. Chem. Phys.* **2018**, *149*, 214503.

(32) Roland, C. M. Characteristic relaxation times and their invariance to thermodynamic conditions. *Soft Matter* **2008**, *4*, 2316–2322.

(33) Coslovich, D.; Roland, C. M. Density scaling in viscous liquids: From relaxation times to four-point susceptibilities. *J. Chem. Phys.* **2009**, *131*, 151103.

(34) Dalle-Ferrier, C.; Thibierge, C.; Alba-Simionesco, C.; Berthier, L.; Biroli, G.; Bouchaud, L. P.; Ladieu, F.; L'Hote, D.; Tarjus, G. Spatial correlations in the dynamics of glassforming liquids: Experimental determination of their temperature dependence. *Phys. Rev. E: Stat., Nonlinear, Soft Matter Phys.* **2007**, *76*, 041510.

(35) Fragiadakis, D.; Roland, C. M. Are polar molecules less simple? *J. Chem. Phys.* **2013**, *138*, 12A502.